THE JOURNAL OF PHYSICAL CHEMISTRY B

Article

Cite This: J. Phys. Chem. B 2018, 122, 2408−2413

pubs.acs.org/JPCB

# Counterion-Regulated Dynamics of Water Confined in Lyotropic Liquid Crystalline Morphologies

Sriteja Mantha,[†] Grayson L. Jackson,[†] Mahesh K. Mahanthappa,[‡] and Arun Yethiraj*[,†]

[†]Department of Chemistry, University of Wisconsin, Madison, Wisconsin 53706, United States

[‡]Department of Chemical Engineering and Materials Science, University of Minnesota, Minneapolis, Minnesota 55455, United States

**ABSTRACT:** The dynamics of confined water is of fundamental and long-standing interest. In technologically important forms of confinement, such as proton-exchange membranes, electrostatic interactions with the confining matrix and counterions play significant roles on the properties of water. There has been recent interest on the dynamics of water confined to the lyotropic liquid crystalline (LLC) morphologies of Gemini dicarboxylate surfactants. These systems are exciting because the nature of confinement, for example, size and curvature of channels and surface functionality is dictated by the chemistry of the self-assembling surfactant molecules. Quasielastic neutron scattering experiments have shown an interesting dependence of the water self-diffusion constant, $D_\alpha$, on the identity (denoted $\alpha$) of the counterion: at high hydration, the magnitude of the water self-diffusion constant is in the order $D_{TMA} < D_{Na} < D_K$, where TMA, Na, and K refer to tetramethyl ammonium, sodium, and potassium counterions, respectively. This sequence is similar to what is seen in bulk electrolyte solutions. At low hydrations, however, the order of water self-diffusion is different, that is, $D_{Na} < D_{TMA} < D_K$. In this work, we present molecular dynamics simulations for the dynamics of water in the LLC phases of dicarboxylate Gemini surfactants. The simulations reproduce the trends seen in experiments. From an analysis of the trajectories, we hypothesize that two competing factors play a role: the volume accessible to the water molecules and the correlations between the water and the counterion. The excluded volume effect is the largest with $TMA^+$, and the electrostatic correlation is the strongest with $Na^+$. The observed trend is a result of which of these two effects is dominant at a given water to surfactant ratio.

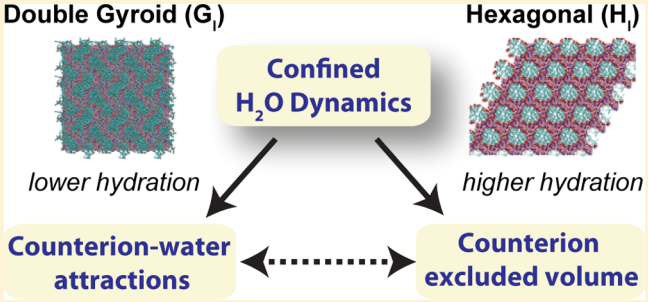


## 1. INTRODUCTION

Understanding the dynamics of water under nanoconfinement is of fundamental and practical importance. The scientific importance arises because properties of confined water can be very different from those in bulk. Surfaces alter the local structure of water in their vicinity,[1−6] and the dynamics of water near a solid surface can be more than an order of magnitude slower than that in the bulk.[7−12] The technological importance arises from the use of nanostructured membranes for proton-exchange applications in, for example, fuel cells. Proton transport is, as one would expect, very sensitive to water dynamics. In this paper, we study, using molecular dynamics simulations, the effect of counterions on the dynamics of water confined in lyotropic liquid crystal (LLC) morphologies formed by surfactant molecules.

There has been recent interest in the lyotropic liquid crystalline (LLC) phases formed by ionic surfactant molecules.[13,14] Surfactant molecules self-assemble into a variety of LLC morphologies.[15−18] The development of new LLC materials through self-assembly is an active area of experimental,[19−31] theoretical,[32−36] and simulation research.[37−49] Interestingly, the chemical natures of the ionic surfactant headgroup and charge compensating counterion are known to effect the aggregation behavior of surfactant molecules[50−54] and properties of confined water.[55−62] Counterions that are closely associated with the surfactant headgroup are shown to favor self-assembled morphologies with flat interfaces (lamellae), whereas those that are more dissociated from the surfactant headgroup favor morphologies with curved interfaces (hexagonally packed cylinders and gyroid).[51,52] These morphologies are depicted in Figure 1.

Jackson et al.[63] have recently measured an interesting counterion-dependent trend in the dynamics of water confined

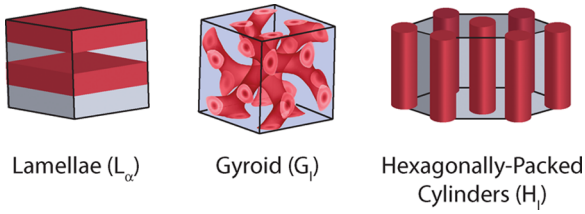


**Figure 1.** Morphologies of dicarboxylate Gemini dicarboxylate surfactants.

**Received:** December 6, 2017
**Revised:** February 1, 2018
**Published:** February 4, 2018







DOI: 10.1021/acs.jpcb.7b12034
J. Phys. Chem. B 2018, 122, 2408−2413

in LLC morphologies formed by self-assembly of anionic Gemini dicarboxylate surfactant molecules with $Na^+$, $K^+$, and tetramethyl ammonium ($TMA^+$) as counterions. Quasielastic neutron scattering experiments were used to obtain the translational self-diffusion coefficient of water as a function of surfactant headgroup/counterion hydration in the LLC phases of Gemini surfactants. The self-diffusion coefficient of water was the highest with the $K^+$ counterion in all cases. However, at low hydration, the diffusion constant was lower with $Na^+$ than with $TMA^+$, and the opposite was true at high hydration.

In this work, we use molecular dynamics simulations to study the counterion-regulated confined water dynamics. Specifically, we explore the effects of $Na^+$, $K^+$, and $TMA^+$ as counterions on the dynamics of water confined in these LLC morphologies at two different ratios of water to surfactant molecules. The simulations reproduced the trends seen in experiments, leading us to derive detailed physical insights into the experimentally observed behavior. We rationalize the results in terms of two competing factors: the volume excluded to water and the interaction between the water and the counterions. The relative importance of these two factors depends on the level of hydration.

## 2. METHODS

The dicarboxylate Gemini surfactant (depicted in Figure 2) has seven methylene groups in the tail and four methylene groups

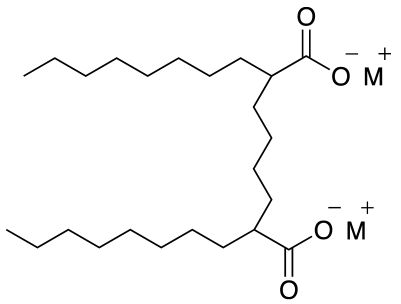


**Figure 2.** Chemical model of the dicarboxylate Gemini surfactants.

in the linker, which are modeled at united atom level using GROMOS45a3 force field.[64] Water molecules are treated at atomistic level using the simple point charge water model. $Na^+$ and $K^+$ ions are modeled at atomistic level,[64,65] and $TMA^+$ ions are modeled at united atom level.[66] Parameters consistent with the water model are used to model interactions with $Na^+$, $K^+$, and $TMA^+$. The force fields are the same as those used in our previous work.[46]

Molecular dynamics simulations are conducted using the GROMACS 4.5.4 simulation package.[67] The simulation parameters are the same as those used in our previous work on Gemini surfactants.[46−49] The Lennard-Jones interactions are switched smoothly to 0 at 1 nm, and the particle mesh Ewald (PME)[68,69] method is used for the Coulomb interactions. The PME parameters are as follows: real space cutoff distance of 1.4 nm and interpolation order of 6, with a maximum fast Fourier transform grid spacing of 0.12 nm. Water molecules are kept rigid using the SETTLE algorithm. The temperature and pressure are maintained using a Berendsen thermostat with coupling time 0.5 ps and a Berendsen barostat with coupling time 1 ps, respectively. The system is propagated using the leapfrog algorithm with a time step of 4 fs.

Initial configurations of self-assembled morphologies are taken from our previous work[46,48] with sodium counterions. Initial configurations for K-74 and TMA-74 are generated by replacing the Na counterions with K or TMA, minimizing the energy of the resulting configuration using a steepest descent algorithm and equilibrating the system at 1 atm and 300 K for 50 ns. This is larger than the equilibration time (typically 10−20 ns) over which the total energy and density reach a steady value. Properties are then averaged over a 300 ns trajectory obtained from simulations at 300 K.

For comparison, we also carry out simulations of concentrated aqueous salt solutions made of $Na^+$, $K^+$, and $TMA^+$ as cations and $Cl^-$ as the anion, using the same force fields. These simulations are equilibrated in the same fashion, but properties are averaged over shorter (10 ns) trajectories generated with a time step of 1 fs.

Simulations for aqueous salt solutions and gyroid (G) morphologies are conducted in a cubic simulation cell, and simulations with hexagonally packed cylindrical (H) morphologies are carried out in a monoclinic box with angle between box vectors set to 90, 90 and 60°.

The parameter, $\lambda$, is defined as the number of water molecules per anionic surfactant headgroup (or anion in the case of the electrolyte solutions). We note that this quantity, $\lambda$, is different from number of water molecules within the first hydration shell around a molecule. We study two levels of hydration, $\lambda$ = 6 and 15, which correspond to a gyroid and hexagonal morphology, respectively. Note that the water dynamics are more sensitive to $\lambda$ than to the morphology.[49] $\lambda$ = 6 is beyond the experimental solubility limit of $Na^+$ and $K^+$ ions. The concentrated aqueous salt solutions in our simulations are stable, and we do not observe any precipitation. Although these systems are not realistic, the comparison with LLC systems at the same hydration provides physical insight into the diffusion mechanism. The systems studied are summarized in Table 1.

## 3. RESULTS AND DISCUSSION

The simulations reproduce the trends seen in experiments. Table 2 lists the ratio of the translation diffusion coefficient to the value of bulk water at the same temperature and pressure as for the systems studied. Diffusion coefficients are computed from the linear region of the mean-squared displacement plot

**Table 1. Parameters for Molecular Dynamics Simulations**

| | | | number of molecules | | | |
|---|---|---|---|---|---|---|
| system | morphology | $\lambda$ | water | surfactant | cations | anions |
| Na-74 | G | 6 | 3000 | 250 | 500 | |
| K-74 | G | 6 | 3000 | 250 | 500 | |
| TMA-74 | G | 6 | 3000 | 250 | 500 | |
| Na-74 | H | 15 | 720 | 24 | 48 | |
| K-74 | H | 15 | 720 | 24 | 48 | |
| TMA-74 | H | 15 | 720 | 24 | 48 | |
| NaCl | | 6 | 930 | | 155 | 155 |
| KCl | | 6 | 930 | | 155 | 155 |
| TMACl | | 6 | 930 | | 155 | 155 |
| NaCl | | 15 | 1160 | | 77 | 77 |
| KCl | | 15 | 1160 | | 77 | 77 |
| TMACl | | 15 | 1160 | | 77 | 77 |



DOI: 10.1021/acs.jpcb.7b12034
J. Phys. Chem. B 2018, 122, 2408−2413

**Table 2. Water Translational Diffusion Coefficients in LLC and Electrolyte Solutions of the Same Ion Concentrations Inversely Relative to That of Pure Water**

| | diffusion coefficient ($D_{bulk}/D$) | | | |
|---|---|---|---|---|
| | $\lambda = 6$ | | $\lambda = 15$ | |
| system | experiment | simulation | experiment | simulation |
| K-74 | 9.7 | 11 | 2.7 | 2.9 |
| Na-74 | 38 | 31 | 3.6 | 4.0 |
| TMA-74 | 33 | 26 | 6.0 | 4.5 |
| KCl | | 2.4 | | 1.5 |
| NaCl | | 3.4 | | 1.8 |
| TMACl | | 11 | | 2.6 |

of water−oxygen atoms generated from the simulation trajectories. (We use $D_{bulk} = 2.299 \times 10^{-5}$ cm$^2$/s for experiment[70,71] and $D_{bulk} = (4.26 \pm 0.06) \times 10^{-5}$ cm$^2$/s for simulations.) The trend $D_{Na} < D_{TMA} < D_K$ for $\lambda = 6$ and $D_{TMA} < D_{Na} < D_K$ for $\lambda = 15$ is seen in both experiment and simulations. Note that the trend at $\lambda = 15$ is similar to what is observed in electrolyte solutions. The values of the diffusion coefficients, however, are much smaller in the LLC systems (than in the electrolyte) because the water is confined and to a greater extent at low ratios of water to surfactant molecules. We believe that the trends are statistically significant because the uncertainties in the simulation results are in the third decimal place.

In all cases, the diffusion constant of water (in LLC and electrolytes) is lower than that in bulk water. There are two factors that could be responsible for this "slowing down" of water. The first is an excluded volume effect, that is, the volume occupied by the counterions decreases the volume accessible to the water molecules. The second is a correlation effect, that is, electrostatic interactions between the water molecules and the counterions cause a dynamic slowing down. We argue that both of these effects play a role but to different degrees depending on the number of water molecules per surfactant.

An estimate of the excluded volume effects can be obtained by considering the fraction of volume (denoted $\phi_w$) available to water molecules. The quantity $\phi_w$ is defined as follows: we calculate the Voronoi volume of every water molecule using the Voro++[73] based code contributed by Abel et al.,[72] add these up to achieve the total volume "occupied" by water, and divide by the volume of the simulation cell to obtain the fraction. Table 3

**Table 3. Fraction of Volume Occupied by Water Molecules ($\phi_w$)**

| | $\phi_w$ | | | |
|---|---|---|---|---|
| | $\lambda = 6$ | | $\lambda = 15$ | |
| counterion | LLC | electrolyte | LLC | electrolyte |
| $Na^+$ | 0.378 | 0.839 | 0.637 | 0.934 |
| $K^+$ | 0.384 | 0.822 | 0.634 | 0.925 |
| $TMA^+$ | 0.345 | 0.643 | 0.579 | 0.808 |

lists $\phi_w$ in the electrolyte and LLC systems. $\phi_w$ is much lower in the LLC systems, of course, because the surfactants occupy a significant portion of the simulation cell volume. The dependence of $\phi_w$ with counterion correlates with the counterion size. In the force fields used, $TMA^+$ has a radius (half of the Lennard-Jones collision diameter) of 0.322 nm, which is more than twice that of $K^+$ (0.152 nm) and $Na^+$ (0.116 nm). Excluded volume effects are clearly greater for $TMA^+$, whereas those for $K^+$ and $Na^+$ are comparable.

An estimate of the correlation effects can be obtained by considering the residence time ($\tau$) of water molecules in the first hydration shell of the various moieties, other water molecules, counterions, and headgroups. Table 4 lists these

**Table 4. Residence Time (in Picosecond) of Water Molecules near Water, Headgroups, and Counterions**

| | water | | | headgroup | | | counterion | | |
|---|---|---|---|---|---|---|---|---|---|
| | $Na^+$ | $K^+$ | $TMA^+$ | $Na^+$ | $K^+$ | $TMA^+$ | $Na^+$ | $K^+$ | $TMA^+$ |
| $\lambda = 6$ | 9 | 5 | 20 | 34 | 23 | 55 | 84 | 18 | 37 |
| $\lambda = 15$ | 5 | 4 | 8 | 17 | 15 | 24 | 45 | 9 | 16 |

residence times, calculated using the algorithm developed by Impey et al.[74] In all cases, the residence time of water around headgroups and counterions is larger than that around other water molecules. It is only reasonable to compare residence times around similarly sized objects because the volume of the first shell is larger for large ions. The results in Table 4 provide a rationalization for why the water dynamics is faster with $K^+$ counterions (compared to that with $Na^+$). The residence time of water near headgroups and counterions is lower with $K^+$ than with $Na^+$ counterions.

The importance of electrostatic correlations can be quantified by comparing the number of water molecules within the first hydration shell (see Table 5) of the counterions to $\lambda$,

**Table 5. Number of Water Molecules within the First Hydration Shell of a Counterion**

| | number of water molecules in the first hydration shell | | | |
|---|---|---|---|---|
| | $\lambda = 6$ | | $\lambda = 15$ | |
| counterion | LLC | electrolyte | LLC | electrolyte |
| $K^+$ | 7.41 | 4.49 | 7.86 | 6.69 |
| $Na^+$ | 4.95 | 2.97 | 5.40 | 4.08 |
| $TMA^+$ | 14.21 | 15.87 | 19.90 | 20.97 |

which is the number of water molecules per headgroup (or counterion). The size of the first hydration shell around a counterion is obtained from the position of the first minimum in the water−oxygen−counterion radial distribution function. In the LLC systems with high hydration ($\lambda = 15$) or in the electrolyte solutions, the number of water molecules in the first hydration shell is much smaller than $\lambda$. This suggests that the fraction of water molecules that are in the first hydration shell is small. In the LLC systems with $\lambda = 6$, however, the number of water molecules within the first hydration shell of $K^+$ and $TMA^+$ is greater than $\lambda$ and that of $Na^+$ is close to $\lambda$. Therefore, the counterion−water correlations are expected to be significant. It is in this regime that we observe the trend $D_{Na} < D_{TMA} < D_K$, which is consistent with electrostatic correlations being important.

The trend (with changing counterions) in the rotational relaxation time (denoted $\tau_R$) of water molecules is independent of hydration, in contrast to the translational diffusion coefficient. The quantity, $\tau_R$, is defined as the time integral of the second-order water dipole moment autocorrelation function. Table 6 lists $\tau_R$ for the different LLC systems studied in this work. The trend $\tau_{R,TMA} > \tau_{R,Na} > \tau_{R,K}$ is seen for systems both at $\lambda = 6$ and at $\lambda = 15$. Such a trend in $\tau_R$ is correlated to



DOI: 10.1021/acs.jpcb.7b12034
J. Phys. Chem. B 2018, 122, 2408−2413

Table 6. Rotational Relaxation Time ($\tau_R$) of Water

| | $\tau_R$/ps | | | |
|---|---|---|---|---|
| | $\lambda$ = 6 | | $\lambda$ = 15 | |
| counterion | LLC | electrolyte | LLC | electrolyte |
| $Na^+$ | 34 | 4 | 4 | 2 |
| $K^+$ | 13 | 2 | 3 | 1 |
| $TMA^+$ | 62 | 17 | 6 | 3 |

that in residence time of water within its hydration shell (refer to data in Table 4). We anticipate that longer relaxation time of water in systems with $TMA^+$ may be due to directional ability of the $TMA^+$ of ordering water molecules.[75,76]

Indeed, the water molecules are more ordered in systems with $TMA^+$ compared to those with $Na^+$ or $K^+$. Figure 3 depicts

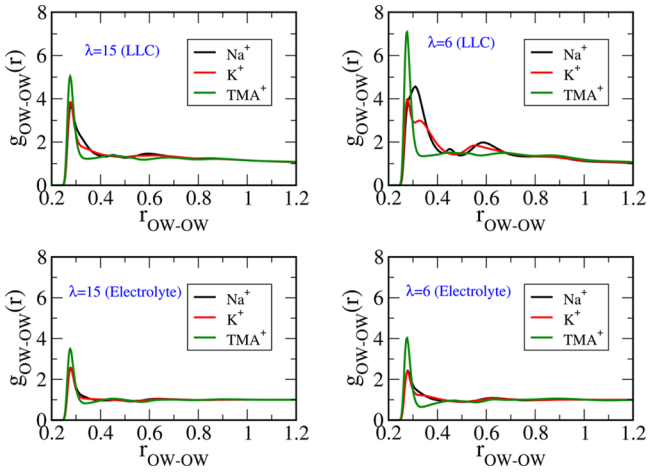


Figure 3. Radial distribution, $g_{OW-OW}(r)$, of water−oxygen around other water−oxygen atoms in different LLC and electrolyte systems.

the radial distribution of water−oxygen around other water−oxygen atoms for the different systems studied in this work. In all cases, the first peak in $g_{OW-OW}(r)$ is very sharp when $TMA^+$ is the counterion. This suggests that there are fewer interstitial water molecules between the first and second hydration shells of a water molecule, that is, the water molecules are more ordered when $TMA^+$ is the counterion.

## 4. SUMMARY

We study the translational diffusion of water in LLC phases of Gemini surfactants using molecular dynamics simulations. Experiments show that the water diffusion constant is sensitive to the identity of the counterion. The diffusion constant is the highest with $K^+$ counterions. At high hydration, the diffusion constant is the lowest with $TMA^+$, and at low hydration, the diffusion constant is the lowest with $Na^+$. The simulations reproduce these trends. We argue that two effects play a role in decreasing the diffusion constant relative to bulk water: the volume excluded to water by the counterions and the correlations between the water and the counterions. The excluded volume is the most important for $TMA^+$, and the correlations are the most important for $Na^+$. The observed trends can be rationalized by noting that correlation effects are more significant at low hydration because a larger fraction of the water molecules is correlated with the counterions.

## AUTHOR INFORMATION


### Corresponding Author

*E-mail: yethiraj@wisc.edu.

### ORCID

Sriteja Mantha: 0000-0001-7813-0903
Grayson L. Jackson: 0000-0003-0663-3274
Mahesh K. Mahanthappa: 0000-0002-9871-804X
Arun Yethiraj: 0000-0002-8579-449X


### Notes

The authors declare no competing financial interest.

## ACKNOWLEDGMENTS

This work was supported by the Department of Energy under award number DE-SC0010328. We acknowledge computational support through Extreme Science and Engineering Discovery Environment (XSEDE) allocations under grant number TG-CHE090065. We acknowledge support from UW-Madison Chemistry Department cluster under grant CHE-0840494 and compute resources and assistance of the UW-Madison Center for High throughput Computing (CHTC).

## REFERENCES


(1) Bruni, F.; Ricci, M. A.; Soper, A. K. Water Confined in Vycor Glass. I. A Neutron Diffraction Study. *J. Chem. Phys.* **1998**, *109*, 1478−1485.

(2) Thompson, H.; Soper, A. K.; Ricci, M. A.; Bruni, F.; Skipper, N. T. The Three-Dimensional Structure of Water Confined in Nanoporous Vycor Glass. *J. Phys. Chem. B* **2007**, *111*, 5610−5620.

(3) Soper, A. K. Radical Re-appraisal of Water Structure in Hydrophilic Confinement. *Chem. Phys. Lett.* **2013**, *590*, 1−15.

(4) Mancinelli, R.; Imberti, S.; Soper, A. K.; Liu, K. H.; Mou, C. Y.; Bruni, F.; Ricci, M. A. Multiscale Approach to the Structural Study of Water Confined in MCM41. *J. Phys. Chem. B* **2009**, *113*, 16169−16177.

(5) Mancinelli, R. The Effect of Confinement on Water Structure. *J. Phys.: Condens. Matter* **2010**, *22*, No. 404213.

(6) Soper, A. K.; Bruni, F.; Ricci, M. A. Water Confined in Vycor Glass. II. Excluded Volume Effects on the Radial Distribution Functions. *J. Chem. Phys.* **1998**, *109*, 1486−1494.

(7) Benham, M. J.; Cook, J. C.; Li, J.-C.; Ross, D. K.; Hall, P. L.; Sarkissian, B. Small-Angle Neutron Scattering Study of Adsorbed Water in Porous Vycor Glass: Supercooling Phase Transition and Interfacial Structure. *Phys. Rev. B* **1989**, *39*, 633−636.

(8) Bellissent-Funel, M.-C.; Chen, S. H.; Zanotti, J.-M. Single-Particle Dynamics of Water Molecules in Confined Space. *Phys. Rev. E* **1995**, *51*, No. 4558.

(9) Rovere, M.; Ricci, M. A.; Vellati, D.; Bruni, F. A Molecular Dynamics Simulation of Water Confined in a cylindrical SiO2 Pore. *J. Chem. Phys.* **1998**, *108*, 9859−9867.

(10) Gallo, P.; Ricci, M. A.; Rovere, M. Layer Analysis of the Structure of Water Confined in Vycor Glass. *J. Chem. Phys.* **2002**, *116*, 342−346.

(11) Rovere, M.; Gallo, P. Effects of Confinement on Static and Dynamical Properties of Water. *Eur. Phys. J. E: Soft Matter Biol. Phys.* **2003**, *12*, 77−81.

(12) Rovere, M.; Gallo, P. Strong Layering Effects and Anomalous Dynamical Behaviour in Confined Water at Low Hydration. *J. Phys.: Condens. Matter* **2003**, *15*, S145.

(13) Kato, T.; Mizoshita, N.; Kishimoto, K. Functional Liquid-Crystalline Assemblies: Self-Organized Soft Materials. *Angew. Chem., Int. Ed.* **2005**, *45*, 38−68.

(14) Hyde, S. In *Handbook of Applied Surface and Colloid Chemistry*; Holmberg, K., Ed.; Wiley: New York, 2001; pp 299−332.




DOI: 10.1021/acs.jpcb.7b12034
J. Phys. Chem. B 2018, 122, 2408−2413

(15) Gin, D. L.; Bara, J. E.; Noble, R. D.; Elliott, B. J. Polymerized Lyotropic Liquid Crystal Assemblies for Membrane Applications. *Macromol. Rapid Commun.* **2008**, *29*, 367−389.
(16) Seddon, J. M. Structure of the Inverted Hexagonal ($H_{II}$) Phase, and Non-Lamellar Phase Transitions of Lipids. *Biochim. Biophys. Acta* **1990**, *1031*, 1−69.
(17) Seddon, J.; Templer, R. In *Structure and Dynamics of Membranes From Cells to Vesicles*; Lipowsky, R., Sackmann, E., Eds.; Handbook of Biological Physics; North- Holland, 1995; Vol. *1*, pp 97−160.
(18) Shearman, G.; Tyler, A.; Brooks, N.; Templer, R.; Ces, O.; Law, R.; Seddon, J. Ordered Micellar and Inverse Micellar Lyotropic Phases. *Liq. Cryst.* **2010**, *37*, 679−694.
(19) Zhou, M.; Nemade, P. R.; Lu, X.; Zeng, X.; Hatakeyama, E. S.; Noble, R. D.; Gin, D. L. New Type of Membrane Material for Water Desalination Based on a Cross-Linked Bicontinuous Cubic Lyotropic Liquid Crystal Assembly. *J. Am. Chem. Soc* **2007**, *129*, 9574−9575.
(20) Gin, D.; Lu, X.; Nemade, P.; Pecinovsky, C.; Xu, Y.; Zhou, M. Recent Advances in the Design of Polymerizable Lyotropic Liquid-Crystal Assemblies for Heterogeneous Catalysis and Selective Separations. *Adv. Funct. Mater.* **2006**, *16*, 865−878.
(21) *Bicontinuous Liquid Crystals*; Lynch, M.; Lynch, M.; Spicer, P., Eds.; Surfactant Science Series; CRC Press: Boca Raton, FL, 2005; pp 1−512.
(22) Spicer, P. T. Progress in Liquid Crystalline Dispersions: Cubosomes. *Curr. Opin. Colloid Interface Sci.* **2005**, *10*, 274−279.
(23) Leal, C.; Bouxsein, N. F.; Ewert, K. K.; Safinya, C. R. Highly Efficient Gene Silencing Activity of siRNA Embedded in a Nanostructured Gyroid Cubic Lipid Matrix. *J. Am. Chem. Soc.* **2010**, *132*, 16841−16847.
(24) Miller, S. A.; Kim, E.; Gray, D. H.; Gin, D. L. Heterogeneous Catalysis with Cross-Linked Lyotropic Liquid Crystal Assemblies: Organic Analogues to Zeolites and Mesoporous Sieves. *Angew. Chem., Int. Ed* **1999**, *38*, 3021−3026.
(25) Jin, J.; Nguyen, V.; Gu, W.; Lu, X.; Elliott, B. J.; Gin, D. L. Cross-Linked Lyotropic Liquid Crystal-Butyl Rubber Composites:? Promising "Breathable" Barrier Materials for Chemical Protection Applications. *Chem. Mater.* **2005**, *17*, 224−226.
(26) Xu, Y.; Gu, W.; Gin, D. L. Heterogeneous Catalysis Using a Nanostructured Solid Acid Resin Based on Lyotropic Liquid Crystals. *J. Am. Chem. Soc* **2004**, *126*, 1616−1617.
(27) Hill, J. P.; Shrestha, L. K.; Ishihara, S.; Ji, Q.; Ariga, K. Self-Assembly: From Amphiphiles to Chromophores and Beyond. *Molecules* **2014**, *19*, 8589.
(28) Wang, C.; Chen, D.; Jiao, X. Lyotropic Liquid Crystal Directed Synthesis of Nanostructured Materials. *Sci. Technol. Adv. Mater.* **2009**, *10*, No. 023001.
(29) Sorenson, G. P.; Coppage, K. L.; Mahanthappa, M. K. Unusually Stable Aqueous Lyotropic Gyroid Phases From Gemini Dicarboxylate Surfactants. *J. Am. Chem. Soc.* **2011**, *133*, 14928−14931.
(30) Sorenson, G. P.; Mahanthappa, M. K. Unexpected Role of Linker Position on Ammonium Gemini Surfactant Lyotropic Gyroid Phase Stability. *Soft Matter* **2016**, *12*, 2408−2415.
(31) Perroni, D. V.; Baez-Cotto, C. M.; Sorenson, G. P.; Mahanthappa, M. K. Linker Length-Dependent Control of Gemini Surfactant Aqueous Lyotropic Gyroid Phase Stability. *J. Phys. Chem. Lett.* **2015**, *6*, 993−998.
(32) Israelachvili, J. N.; Mitchell, D. J.; Ninham, B. W. Theory of Self-Assembly of Hydrocarbon Amphiphiles into Micelles and Bilayers. *J. Chem. Soc., Faraday Trans. 2* **1976**, *72*, 1525−1568.
(33) Gunnarsson, G.; Joensson, B.; Wennerstroem, H. Surfactant Association into Micelles. An Electrostatic Approach. *J. Phys. Chem.* **1980**, *84*, 3114−3121.
(34) Nagarajan, R.; Ruckenstein, E. Theory of Surfactant Self-assembly: A Predictive Molecular Thermodynamic Approach. *Langmuir* **1991**, *7*, 2934−2969.
(35) Diamant, H.; Andelman, D. Free Energy Approach to Micellization and Aggregation: Equilibrium, Metastability, and Kinetics. *Curr. Opin. Colloid Interface Sci.* **2016**, *22*, 94−98.
(36) Hines, J. Theoretical Aspects of Micellisation in Surfactant Mixtures. *Curr. Opin. Colloid Interface Sci.* **2001**, *6*, 350−356.
(37) Smit, B.; Esselink, K.; Hilbers, P. A. J.; Van Os, N. M.; Rupert, L. A. M.; Szleifer, I. Computer Simulations of Surfactant Self-assembly. *Langmuir* **1993**, *9*, 9−11.
(38) Karaborni, S.; Smit, B. Computer Simulations of Surfactant Structures. *Curr. Opin. Colloid Interface Sci.* **1996**, *1*, 411−415.
(39) Klein, M. L.; Shinoda, W. Large-Scale Molecular Dynamics Simulations of Self-Assembling Systems. *Science* **2008**, *321*, 798−800.
(40) Rajagopalan, R. Simulations of Self-assembling Systems. *Curr. Opin. Colloid Interface Sci.* **2001**, *6*, 357−365.
(41) LeBard, D. N.; Levine, B. G.; Mertmann, P.; Barr, S. A.; Jusufi, A.; Sanders, S.; Klein, M. L.; Panagiotopoulos, A. Z. Self-assembly of Coarse-grained Ionic Surfactants Accelerated by Graphics Processing Units. *Soft Matter* **2012**, *8*, 2385−2397.
(42) Wang, Z.; Le, P.; Ito, K.; Leão, J. B.; Tyagi, M.; Chen, S.-H. Dynamic Crossover in Deeply Cooled Water Confined in MCM-41 at 4 kbar and its Relation to the Liquid-Liquid Transition Hypothesis. *J. Chem. Phys.* **2015**, *143*, No. 114508.
(43) Suttipong, M.; Grady, B. P.; Striolo, A. Self-assembled Surfactants on Patterned Surfaces: Confinement and Cooperative Effects on Aggregate Morphology. *Phys. Chem. Chem. Phys.* **2014**, *16*, 16388−16398.
(44) Jusufi, A.; Kohlmeyer, A.; Sztucki, M.; Narayanan, T.; Ballauff, M. Self-Assembly of Charged Surfactants: Full Comparison of Molecular Simulations and Scattering Experiments. *Langmuir* **2012**, *28*, 17632−17641.
(45) He, X.; Wataru, S.; Russell, D.; Kelly, L. A.; Klein, M. L. Paramaterization of a Coarse-grained Model for Linear Alkylbenzene Sulfonate Surfactants and Molecular Dynamics Studies of Their Self-Assembly in Aqueous Solution. *Chem. Phys. Lett.* **2010**, *487*, 71−76.
(46) Mondal, J.; Mahanthappa, M. K.; Yethiraj, A. Self-Assembly of Gemini Surfactants: A Computer Simulation Study. *J. Phys. Chem. B* **2013**, *117*, 4254−4262.
(47) Mantha, S.; Yethiraj, A. Dynamics of Water Confined in Lyotropic Liquid Crystals: Molecular Dynamics Simulations of the Dynamic Structure Factor. *J. Chem. Phys.* **2016**, *144*, No. 084504.
(48) Mantha, S.; McDaniel, J. G.; Perroni, D. V.; Mahanthappa, M. K.; Yethiraj, A. Electrostatic Interactions Govern "Odd-Even" Effects in Water-Induced Gemini Surfactant Self-assembly. *J. Phys. Chem. B* **2017**, *121*, 565−576.
(49) McDaniel, J. G.; Mantha, S.; Yethiraj, A. Dynamics of Water in Gemini Surfactant-Based Lyotropic Liquid Crystals. *J. Phys. Chem. B* **2016**, *120*, 10860−10868.
(50) Liu, C. K.; Warr, G. G. Self-Assembly of Didodecyldimethylammonium Surfactants Modulated by Multivalent, Hydrolyzable Counterions. *Langmuir* **2015**, *31*, 2936−2945.
(51) Liu, C. K.; Warr, G. G. Resiliently Spherical Micelles of Alkyltrimethylammonium Surfactants with Multivalent, Hydrolyzable Counterions. *Langmuir* **2012**, *28*, 11007−11016.
(52) Liu, C. K.; Warr, G. G. Hexagonal Closest-Packed Spheres Liquid Crystalline Phases Stabilised by Strongly Hydrated Counterions. *Soft Matter* **2014**, *10*, 83−87.
(53) Berr, S.; Jones, R. R. M.; Johnson, J. S. Effect of Counterion on the Size and Charge of Alkyltrimethylammonium Halide Micelles as a Function of Chain Length and Concentration as Determined by Small Angle Neutron Scattering. *J. Phys. Chem.* **1992**, *96*, 5611−5614.
(54) Brady, J. E.; Evans, D. F.; Warr, G. G.; Grieser, F.; Ninham, B. W. Counterion Specificity as the Determinant of Surfactant Aggregation. *J. Phys. Chem.* **1986**, *90*, 1853−1859.
(55) Riter, R. E.; Undiks, E. P.; Levinger, N. E. Impact of Counterion on Water Motion in Aerosol OT Reverse Micelles. *J. Am. Chem. Soc.* **1998**, *120*, 6062−6067.
(56) Park, S.; Moilanen, D. E.; Fayer, M. D. Water Dynamics: The Effects of Ions and Nanoconfinement. *J. Phys. Chem. B* **2008**, *112*, 5279−5290.
(57) Ladanyi, B. M. Computer Simulation Studies of Counterion Effects on the Properties of Surfactant Systems. *Curr. Opin. Colloid Interface Sci.* **2013**, *18*, 15−25.


DOI: 10.1021/acs.jpcb.7b12034
*J. Phys. Chem. B* 2018, 122, 2408−2413

(58) Harpham, M. R.; Ladanyi, B. M.; Levinger, N. E. The Effect of the Counterion on Water Mobility in Reverse Micelles Studied by Molecular Dynamics Simulations. *J. Phys. Chem. B* **2005**, *109*, 16891−16900.
(59) Senapati, S.; Berkowitz, M. L. Computer Simulation Studies of Water States in Perfluoro Polyether Reverse Micelles:? Effects of Changing the Counterion. *J. Phys. Chem. A* **2004**, *108*, 9768−9776.
(60) Faeder, J.; Albert, M. V.; Ladanyi, B. M. Molecular Dynamics Simulations of the Interior of Aqueous Reverse Micelles:? A Comparison between Sodium and Potassium Counterions. *Langmuir* **2003**, *19*, 2514−2520.
(61) Pant, D.; Riter, R. E.; Levinger, N. E. Influence of Restricted Environment and Ionic Interactions on Water Solvation Dynamics. *J. Chem. Phys.* **1998**, *109*, 9995−10003.
(62) Moilanen, D. E.; Levinger, N. E.; Spry, D. B.; Fayer, M. D. Confinement or the Nature of the Interface? Dynamics of Nanoscopic Water. *J. Am. Chem. Soc.* **2007**, *129*, 14311−14318.
(63) Jackson, G. L.; Mantha, S.; Kim, S.; Diallo, S. O.; Herwig, K. W.; Yethiraj, A.; Mahanthappa, M. K. Ion-specific Confined Water Dynamics in Convex Nanopores of Lyotropic Liquid Crystals. *J. Phys. Chem. B* **2017**, submitted for publication.
(64) Schuler, L. D.; Daura, X.; van Gunsteren, W. F. An Improved GROMOS96 Force Field for Aliphatic Hydrocarbons in the Condensed Phase. *J. Comput. Chem* **2001**, *22*, 1205−1218.
(65) Dang, L. X. Mechanism and Thermodynamics of Ion Selectivity in Aqueous Solutions of 18-Crown-6 Ether: A Molecular Dynamics Study. *J. Am. Chem. Soc.* **1995**, *117*, 6954−6960.
(66) Reif, M. M.; Hünenberger, P. H.; Oostenbrink, C. New Interaction Parameters for Charged Amino Acid Side Chains in the GROMOS Force Field. *J. Chem. Theory Comput.* **2012**, *8*, 3705−3723.
(67) Hess, B.; Kutzner, C.; Van der Spoel, D.; Lindahl, E. GROMACS 4:? Algorithms for Highly Efficient, Load-Balanced, and Scalable Molecular Simulation. *J. Chem. Theory Comput.* **2008**, *4*, 435.
(68) Darden, T.; York, D.; Pedersen, L. Particle Mesh Ewald: An Nlog(N) Method for Ewald Sums in Large Systems. *J. Chem. Phys.* **1993**, *98*, 10089−10092.
(69) Essmann, U.; Perera, L.; Berkowitz, M. L.; Darden, T.; Lee, H.; Pedersen, L. G. A Smooth Particle Mesh Ewald Method. *J. Chem. Phys* **1995**, *103*, 8577−8593.
(70) Mills, R. Self-Diffusion in Normal and Heavy Water in the Range 1−45.deg. *J. Phys. Chem.* **1973**, *77*, 685−688.
(71) Holz, M.; Heil, S. R.; Sacco, A. Temperature-Dependent Self-Diffusion Coefficients of Water and Six Selected Molecular Liquids for Calibration in Accurate 1H NMR PFG Measurements. *Phys. Chem. Chem. Phys.* **2000**, *2*, 4740−4742.
(72) Abel, S.; Dupradeau, F.-Y.; Marchi, M. Molecular Dynamics Simulations of a Characteristic DPC Micelle in Water. *J. Chem. Theory Comput.* **2012**, *8*, 4610−4623.
(73) Rycroft, C. H. VORO++: A Three-Dimensional Voronoi Cell Library in C++. *Chaos* **2009**, *19*, No. 041111.
(74) Impey, R. W.; Madden, P. A.; McDonald, I. R. Hydration and Mobility of Ions in Solution. *J. Phys. Chem.* **1983**, *87*, 5071−5083.
(75) García-Tarrés, L.; Guardia, E. Hydration and Dynamics of a Tetramethylammonium Ion in Water:? A Computer Simulation Study. *J. Phys. Chem. B* **1998**, *102*, 7448−7454.
(76) Bhowmik, D.; Malikova, N.; Meriguet, G.; Bernard, O.; Teixeira, J.; Turq, P. Aqueous Solutions of Tetraalkylammonium Halides: Ion Hydration, Dynamics and Ion-Ion Interactions in Light of Steric Effects. *Phys. Chem. Chem. Phys.* **2014**, *16*, 13447−13457.



DOI: 10.1021/acs.jpcb.7b12034
*J. Phys. Chem. B* 2018, 122, 2408−2413